Cochlear implants: Modeling electrophysiological responses

Gendt, M.J. van

CHAPTER 5

Effect of neural adaptation and degeneration on pulse-train eCAPs: a model study

Margriet J. van Gendt
Jeroen J. Briaire
Johan H.M. Frijns

Hearing Research (2019) 377, 167-178

Abstract

Electrically evoked compound action potentials (eCAPs) are measurements of the auditory nerve's response to electrical stimulation. ECAP amplitudes during pulse trains can exhibit temporal alternations. The magnitude of this alternation tends to diminish over time during the stimulus. How this pattern relates to the temporal behavior of nerve fibers is not known. We hypothesized that the stochasticity, refractoriness, adaptation of the threshold and spike-times influence pulse-train eCAP responses. Thirty thousand auditory nerve fibers were modeled in a three-dimensional cochlear model incorporating pulse-shape effects, pulse-history effects, and stochasticity in the individual neural responses. ECAPs in response to pulse trains of different rates and amplitudes were modeled for fibers with different stochastic properties (by variation of the relative spread) and different temporal properties (by variation of the refractory periods, adaptation and latency). The model predicts alternation of peak amplitudes similar to available human data. In addition, the peak alternation was affected by changing the refractoriness, adaptation, and relative spread of auditory nerve fibers. As these parameters are related to factors such as the duration of deafness and neural survival, this study suggests that the eCAP pattern in response to pulse trains could be used to assess the underlying temporal and stochastic behavior of the auditory nerve. As these properties affect the nerve's response to pulse trains, they are of uttermost importance to sound perception with cochlear implants.

1 Introduction

Electrically evoked compound action potentials (eCAPs) arise from the auditory nerve's response to electrical stimulation. ECAPs are often measured in cochlear implant (CI) recipients, the clinical applicability is widely studied (e.g. Al Muhaimeed et al., 2010; Hughes et al., 2000; Mittal and Panwar, 2009) and for a review see de Vos et al. (2017). In the most conventional eCAP measurements, a forward masking paradigm is used to obtain information about the neural response to a single pulse. The N1-P2 peak in that response provides insight into the number and location of fibers firing in response to the given stimulus. In a different approach (Wilson et al., 1994), the neural response to a train of pulses can be measured, an example of which is shown in figure 5.1 (Hughes et al., 2012). In the present study, this type of measurement is replicated using a comprehensive computational model.

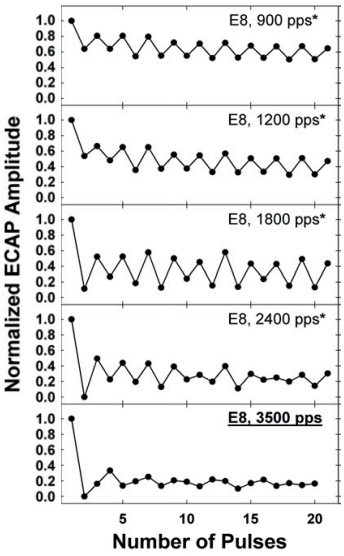

Figure 5.1. Human eCAP data in response to constant amplitude pulse trains (Hughes et al., 2012) Reprinted with permission.

eCAP measurements in response to pulse trains were first performed in humans by Wilson et al. (1994), who showed alternating eCAP amplitudes in response to certain stimulation rates. Such responses to pulse trains with rates up to 4000 pps were then studied in several groups of CI users (figure 5.1) (Hughes et al., 2014, 2012; Wilson et al., 1997, 1994). This alternation pattern is most clearly seen at rates of 1000-2000 pps and is thought to be an effect of refractoriness and membrane noise. At higher rates, the alternating pattern disappears, probably due to asynchronous firing. The rate at which the alternation disappears is sometimes referred to as the stochastic resonance frequency.

This was hypothesized to be a desirable state of the auditory nerve as the nerve then may be sensitive to small input fluctuations, and could be obtained by including a noise conditioner (Rubinstein et al., 1999). Overall eCAP amplitudes decrease at higher pulse rates , which is thought to be related to adaptation and accommodation (Cohen, 2009; Hay-McCutcheon et al., 2005; Schmidt, Clay, and Brown, 2007). Animal studies show similar behavior of the pulse-train eCAP (Abbas et al., 1999; Campbell et al., 2012; Haenggeli et al., 1998; Jeng et al., 2009; Loquet et al., 2004; Matsuoka et al., 2000; Ramekers et al., 2015).

Several researchers have attempted to correlate the pulse-train eCAP in response to psychophysical measures of temporal processing (e.g., gap detection, pitch perception, and loudness summation) or speech perception (Hay-McCutcheon et al., 2005; Huarte et al., 2014; Hughes et al., 2014; McKay et al., 2013; Zhang et al., 2013). Better pitch perception was shown to be related to lower alternations in responses (Carlyon and Deeks, 2015). There is however a large inter-patient variability in the eCAP alternation and correlations with psychophysical measures, which therefore up to this date remains a subject of debate.

As sensorineural hearing loss results in a reduction in the spiral ganglion cell population and demyelination of the peripheral dendrites up to the central axon (Leake and Hradek, 1988), differences in morphology and physiology of auditory neurons may be a major cause of the variable outcomes observed in CI users. Hearing loss and altered neural refractoriness have been shown to occur concomitantly. Ramekers et al. (2015) studied the effect of deafness on the eCAP response to pulse trains, comparing eCAP data to histology. Pulse-train eCAP responses in deafened animals showed an increase in normalized eCAP amplitude and eCAP alternation at specific rates at the end of 100-ms stimulation. The time course of SGN degeneration after deafness seems to be species-dependent (Kalkman et al., 2016). For instance, in cats, Leake and Hradek et al. (1988) showed continuous degeneration of spiral ganglion neurons, which could progress over up to several years, following administration of ototoxic drugs. On the contrary, in humans a gradually degeneration of the peripheral processes is suggested, where possibly after long duration deafness only the unmyelinated terminal disappears (Snel-Bongers et al., 2013).

Though most research on pulse-train eCAPs has focused on constant-amplitude pulse trains, some studies have measured responses to amplitude-modulated input, both in humans and animals (Abbas et al., 1999; Jeng et al., 2009; Tejani et al., 2017; Wilson et al., 1997, 1994). Such measurements are relevant to contemporary CIs, which encode speech by transferring the envelope and amplitude modulations in the speech signal. Tejani et al. (2017) found an increased modulated response amplitude (MRA) with increased modulation frequency, attributing this to neural adaptation. The MRA was defined as the average difference between the minimal and maximal eCAP response over one modulation cycle. Comparing the MRA to the modulation detection thresholds in the same patients revealed a trend of better modulation detection, with larger MRA in the lower frequencies, indicating a potential role for a central limiting factor. A comprehensive

neural model could be used to test and better understand the effect of these modulation depths, as well as the effects of other parameters, such as neural adaptation and stimulus amplitude, on MRA.

Biophysical models can reproduce the effect of stimulus parameters on auditory neurons (Dekker et al., 2014; Frijns and ten Kate, 1994; Mino et al., 2004; Reilly et al., 1985; Resnick et al., 2018; Woo et al., 2009). However, modeling the response of large numbers of auditory nerve fibers to pulse trains requires a lot of computational power. To reduce computational demands, phenomenological models have been developed to predict eCAP responses to sustained stimulation. These models have included stochastic and temporal behavior (I. C. Bruce et al., 1999; Chen and Zhang, 2007; Macherey et al., 2007; van Gendt et al., 2017, 2016; Xu and Collins, 2007). Previous modeling work has shown that the alternating pattern may be produced by interactions between refractoriness and stimulus rate. For short-duration stimuli, a model that includes latency, jitter, membrane stochasticity, and refractoriness predicts human responses very well (Hamacher, 2004; Matsuoka et al., 2000; Rubinstein, 1995; Wilson et al., 1994). Membrane stochasticity is described by the relative spread parameter (RS). RS is defined as the standard deviation of the Gaussian distribution of thresholds divided by its mean (Verveen and Derksen, 1968). Simulations showed, depending on the stimulus rate, a smaller alternation depth with larger RS. Campbell et al. (2012) found that inclusion of adaptation removed the overestimation of probability of firing after a longer duration of stimulation. Thus, patterns in the eCAP response to pulse trains provide insights into the temporal behavior of the auditory nerve. Our biophysical model is the first that combines pulse shape, geometry of current spread, a realistic number of auditory neurons, and phenomenological stochastic parameters of short-term and long-term behavior. By combining this with a unitary response, we were able to reproduce human whole-nerve responses to pulse trains.

The goal of this study was twofold; firstly to validate the previously published model (van Gendt et al., 2017, 2016) with human data, and secondly to investigate the effect of neural parameters on the pulse-train eCAP. The investigated neural parameters were adaptation and accommodation, refractoriness, relative spread, jitter, and the number of fibers, which are important for sound perception with a cochlear implant. By using a model of the auditory nerve's response to CI stimulation we try to understand the origin of the pulse-train eCAP response, inter-patient variability in those responses, their relationship with psychophysical measurements, and the effect of hearing loss on these responses. We hypothesize that neural degeneration may be related to abnormal refractoriness and adaptation, and that the effect of both refractoriness and adaptation are visible in the pulse-train eCAP responses.

2 Methods

2.1 Model

eCAP responses to constant-amplitude and amplitude-modulated pulse trains produced and detected with a CI were simulated. The modeled nerve consisted of 32,000 stochastically independent neural fibers at 3200 different spatial locations. Electric-field spread of the stimulus and its effect on neural thresholds was calculated using the three-dimensional volume conduction model and an active nerve fiber model (Frijns et al., 1995; Kalkman et al., 2015, 2014). This model was extended with empirical parameters for refractoriness, membrane stochasticity, adaptation, and accommodation based on single-fiber animal studies (van Gendt et al., 2017, 2016). For each fiber, all phenomenological parameters were chosen randomly from a pre-defined normal distribution as described by van Gendt et al. (2016, 2017). Deterministic thresholds were obtained for single pulses with specific pulse shapes and pulse widths. The accommodation parameter is dependent on the pulse width. Monopolar biphasic pulses with a pulse duration of 25 µs were used for the simulations. The 1J electrode array with 16 electrode contacts was placed in the model. The electrode contact located roughly 180° from the round window was stimulated. Figure 5.2 shows the threshold profile related to this electrode based on the thresholds from the deterministic model for each fiber. A description of the complete model and validation for single fiber responses to constant-amplitude and amplitude-modulated pulse trains can be found in previously published papers (van Gendt et al., 2017, 2016). In addition to the previously used parameters, a spike time latency was implemented, with the mean latency value referring to the delay between stimulus and spike, and with the jitter value referring to the standard deviation of the latency.

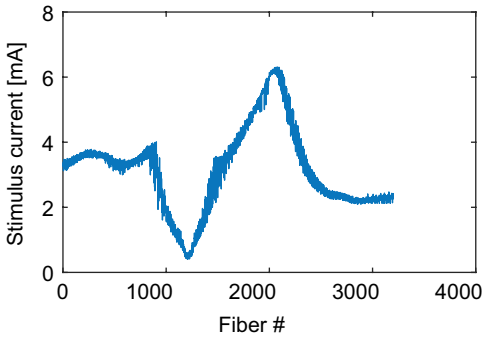

Figure 5.2. Threshold profile for electrode 8 (located 180˚ from the round window). The line shows the threshold for each individual fiber. Pulse-width used is 25 µs. The fibers have equidistant locations along the basilar membrane. Location #1 refers to the fiber closest to the round window, #3200 is the most apically located fiber.

The model is validated to predict spike timings of neurons in response to pulse trains (van Gendt et al., 2017, 2016). To calculate the eCAP responses, these predicted pulse timings were convolved with an estimation of the unitary response (Miller et al., 1999b). This unitary response was derived using the method proposed by Goldstein and Kiang (1958), who assumed that the eCAP(t) is a convolution of the compound PST histogram, P(t), and the unitary response U(t) as described in equation 5.1;

$$eCAP(t) = \int_{-\infty}^{t} P(\tau) \cdot U(t-\tau)\ d\tau \qquad \text{(Eq. 5.1)}$$

The unitary response was obtained by deconvolving a typical eCAP waveform with a modeled post-stimulus time (PST) histogram, assuming an equal contribution of all fibers to the neural eCAP (Miller et al., 1999b). The current paper uses Miller et al.'s unitary response based on a cat's eCAP response to a monophasic anodic pulse of 39 µs and based on the assumption that all fibers contribute equally to the response. This latter assumption is validated by studies showing that fiber diameters of different regions of cochlear innervation are comparable (Arnesen and Osen, 1978; Liberman and Oliver, 1984). Figure 5.3 shows the predicted unitary response as included in the current model (Miller et al., 1999b). The shape of the unitary response is a scaled version of the eCAP waveform.

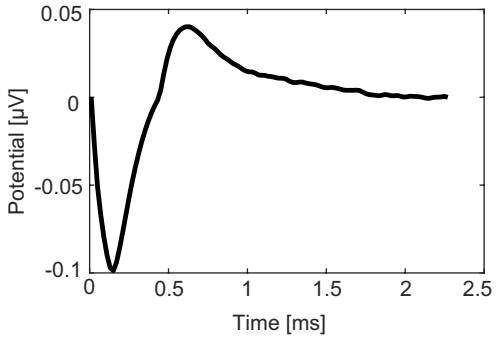

Figure 5.3. Unitary response used in the simulations (after Miller et al., 1999). Since a unitary response is assumed, the y-axis is directly proportional to the eCAP amplitude.

This unitary response is subsequently convolved with all our predicted spike timings per fiber R (t) and the resulting response in time is summed over all fibers (f), as described in equation 5.2;

$$eCAP(t) = \sum_{f=1}^{32000} \sum_{\tau=-\infty}^{t} R\ (t)\ U(t-\tau)\ d\tau\ df \qquad \text{(Eq. 5.2)}$$

2.2 Stimulus levels

To investigate the effect of stimulus level on the eCAP response the stimulus levels were varied; levels of 1.2, 1.5 and 1.8 mA were used. Figure 5.4 shows the growth in neural recruitment with stimulus level for different rates. The initial (deterministic) thresholds are determined by the 3D volume conduction and the cable model (Kalkman et al., 2014). In the deterministic model, threshold and most comfortable loudness levels are defined by the number of excited neurons, based on observations in current steering experiments (Snel-Bongers et al., 2013). This corresponds to 1- and 4-mm excitation along the basilar membrane in the 3D cochlear model, which in our current model corresponds to 1000 and 4000 excited neurons.

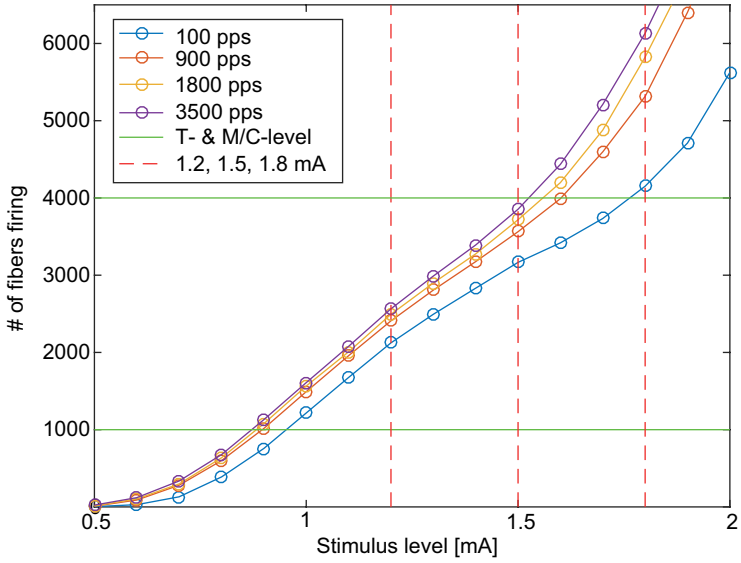

Figure 5.4. total number of fibers firing in response to a 150-ms pulse train for pulse rates from 100 to 3500 pps. The green solid lines show where the T- (1000 fibers, 1mm, see explanation in section 2.2) and M/C (4000 fibers, 4mm, see explanation in section 2.2). The red dotted lines indicate stimulus levels used in the other stimulations.

Despite the fact that the parameters are chosen within physiological boundaries, the resulting predicted thresholds of the neural cable model are much higher than those seen in patients, which is a known issue in cable models (Kalkman et al., 2016). Thus, while single-fiber electrophysiological recordings are well predicted, there are discrepancies with whole nerve recordings, which are not yet understood. Absolute stimulus levels used in our model can therefore not be quantitatively related to those used in patient studies, but we can interpret the levels in terms of the dynamic range (the stimulus level relative to T- and M/C-levels).

2.3 Variation of model parameters

The model was validated by comparing its output in response to pulse trains with existing human data using the standard parameters shown in table 5.1. To investigate the effect of adaptation, refractoriness, relative spread, and the number of functional fibers on the eCAP responses to pulse trains, model parameters were varied as shown in table 5.1. The values for RS and refractory periods were based on literature. Animal experiments have shown that RS is dependent on pulse shape and ranged from 0.07 ± 0.07 for monophasic to 0.12 ± 0.06 for biphasic pulse shapes, all measured in cats (Bruce et al., 1999b; Javel et al., 1987; Miller et al., 1999a). To investigate both the average and very extreme cases, we have chosen to set the RS to 0.06 ± 0.04 in the standard parameter setting, and to 0.0 ± 0.0 and 0.12 ± 0.08 in the extreme ranges. For refractoriness, the absolute refractory period (ARP) and the relative refractory period (RRP), data are available from animal experiments combined with computational modeling (Dynes, 1996; Miller et al., 2001). Estimated ARP values ranged from 0.3 ± 0.1 (Miller et al., 2001) to 0.7 ms (Dynes, 1996) and RRP values from 0.4 ± 0.2 to 1.32. These extreme values were all characterized in cats. For humans, values were around 0.7 ms based on eCAPs by using an exponential fit (Cartee et al., 2000). To cover the whole range of experimental data, our average parameter settings for ARP and RRP were set to 0.4 ± 0.1 and 0.8 ± 0.5 respectively, whereas for the extremes these values were multiplied by 0.5 and 1.5, resulting in ARP and RRP values of 0.2 ± 0.05 and 0.4 ± 0.25 for the low refractory and 0.6 ± 0.15 and 1.2 ± 0.75 for the high refractory case.

The standard adaptation and accommodation values were all based on our previous modeling work (van Gendt et al., 2017, 2016), where these values were derived by comparison of the model output with published animal data (Litvak et al., 2001; Miller et al., 2008; Zhang et al., 2007). To investigate the necessity of including adaptation and accommodation in a model of cochlear implant stimulation, the model was also run without these effects. To test the sensitivity of the response to the chosen values, the parameters were varied to the extreme high adaptation/accommodation scenario. These extreme values are double the average values, chosen as such because of the large standard deviation on the adaptation parameter as determined in the previous modeling work.

The model has 32,000 fibers, which closely matches the number of type I auditory nerve fibers in the normal-hearing human situation. As an extreme case of neural degeneration a uniformly distributed neural survival of 10% was chosen. In some simulations jitter and latency were implemented using the parameters reported in cats (Miller et al., 1999a). For the simulations, both constant-amplitude and amplitude-modulated pulse trains were used.

Table 5.1. Model parameter variations.RS = relative spread, ARP = absolute refractory period, RRP = relative refractory period, Adap = adaptation, Acco = accommodation, # fbrs = number of fibers, Lat = latency, Jit = jitter

	RS	ARP, ms	RRP, ms	Adap	Acco	# fbrs	Lat, ms	Jit, ms
Standard	0.06 ± 0.04	0.4 ± 0.1	0.8 ± 0.5	1 ± 0.6	0.03	32,000	0	0
Low	0	0.2 ± 0.05	0.4 ± 0.25	0	0	3200	-	-
High	0.12 ± 0.08	0.6 ± 0.15	1.2 ± 0.75	2 ± 1.2	0.06	-	0.7	0.07

Experiment A: short-duration pulse trains

To validate the model with human data, human recordings as published by Hughes et al. (2012) were simulated with standard parameter settings as listed in row 1 of table 5.1. To evaluate the effect of neural parameters these simulations were replicated with the model parameters as indicated in rows 2 and 3 of table 5.1. In each of these simulations, one parameter was varied to either the low or high extreme value. To replicate the recordings by Hughes et al., constant-amplitude pulse trains with rates of 900, 1200, 1800, 2400, and 3500 pps were used. Stimulus amplitude was set to 1.5 mA. The effect of neural degeneration was tested by comparing 10% neural survival distributed evenly over the cochlea with the 100% neural survival situation (32,000 fibers). Responses to the first 20 pulses were simulated, the total stimulus duration was thus dependent on the rate. Results were normalized to the amplitude obtained in response to the first pulse. The alternation depth was calculated as the difference between the average normalized response to the odd and even pulses from pulse numbers 2 to 21.

Experiment B: short-duration, low-rate pulse trains

eCAPs in response to 100-ms, low-rate, pulse trains as measured in CI listeners by Carlyon and Deeks (2015) were simulated for comparison to human data and to investigate the effect of neural parameters and stimulus amplitude. Alternation depth was defined as the ratio between the responses to the odd and even pulse numbers. Responses to stimulation rates of 100, 130, 200, 270, 300, 400, and 500 pps were simulated, and stimulus levels of 1.2 and 1.5 mA were used. For the stimulus amplitude of 1.2 mA, varying model settings were evaluated. In the experiments done by Carlyon and Deeks (2015) stimulation rates up to 500 pps were used, whereas in the experiments by Hughes et al. (2012) rates of 900 pps and higher were used. To investigate whether the simulations of the two studies would have been the same when the same rates were used, the simulations were repeated with a stimulus rate of 900 pps.

Experiment C: long-duration pulse trains

Predicted eCAP responses to 100-ms pulse trains were compared to animal data published by Ramekers et al. (2015) in order to investigate the temporal and stochastic effects on responses to longer duration pulse trains. Stimulus rates were set to 125, 250, 500, 625, 1250, 1667, and 2500 pps. The stimulus amplitude was 1.2 mA. The responses were predicted with the standard parameter settings and the parameter variations listed in table 5.1. Uniformly distributed neural survival rates of 100% and 10% were tested.

Experiment D: amplitude-modulated pulse trains

Responses to 100-ms amplitude-modulated pulse trains were simulated and compared to previously published animal data (Jeng et al., 2009). The amplitude used was 1.5 mA, and different model parameter settings were evaluated. The modulation depth was set to 10% and modulation frequency to 25, 50, 100, 200, 300, and 400 Hz. The carrier rate was 1000 pps.

Experiment E: Short-duration amplitude-modulated pulse trains

Responses to 15-ms amplitude-modulated pulse trains were simulated and the resulting modulation response amplitudes compared to published human data (Tejani et al., 2017). Stimulus amplitudes of 1.5- and 1.8-mA were used to mimic patient measurements. At the lowest amplitude and 30% modulation depth, both complete and partial (10%) neural survival was simulated. Full nerve simulations were performed with all parameter settings as shown in table 5.1. The modulation depth was set to 10%, 20%, and 30% and modulation frequency varied to 125, 250, 500, and 1000 Hz. As in the experiments with humans, the carrier rate was 4000 pps. Tejani's detection of modulation as a function of MRA was used to evaluate the modulation following behavior, with a larger MRA implying increased modulation following behavior of the auditory nerve. These simulations were performed to investigate whether the modulation following behavior was determined mostly by stimulus parameters, or by the neural properties as suggested by Tejani et al.

3 Results

3.1 Experiment A: Short-duration pulse trains

The responses to short-duration pulse trains are shown in figures 5.5 and 5.6, with summary data shown in table 5.2. Simulated eCAP responses obtained with four different model settings when stimulated with pulse trains of 1.5 mA are shown in figure 5.5. Removal of adaptation did not change the auditory nerve's response to this stimulation. With a shorter refractory period, the alternation pattern was stronger at higher stimulus rates, and the decrease in average response amplitude from the first to the last pulse was somewhat smaller for all rates than when standard parameter settings were used. Removal of RS, i.e., making the fibers deterministic, led to enhanced alternation and did not affect the preferred stimulation rate for alternation. With lower stimulus amplitudes (data not shown), similar behavior was observed, though a slightly larger relative decrease occurred quickly after the onset of stimulation at the lowest two rates. When only 10% of the fibers were modeled, the results were very similar to when 100% of the neurons were included in the model and are therefore not plotted.

Table 5.2. Summary of the effects of each model perturbation on both the eCAP alternation depth and the eCAP response amplitude, as shown in more detail in figure 5.6;

Model perturbation:	eCAP alternation depth:	eCAP response amplitude:
Short refractoriness	Decrease for low rates Increase for high rates	Increase
Long refractoriness	Minor decrease at rates 1200 & 1800 pps	Decrease
Deterministic	Increase	Minor decrease
High RS	Minor decrease at rate 900 pps	Minor increase

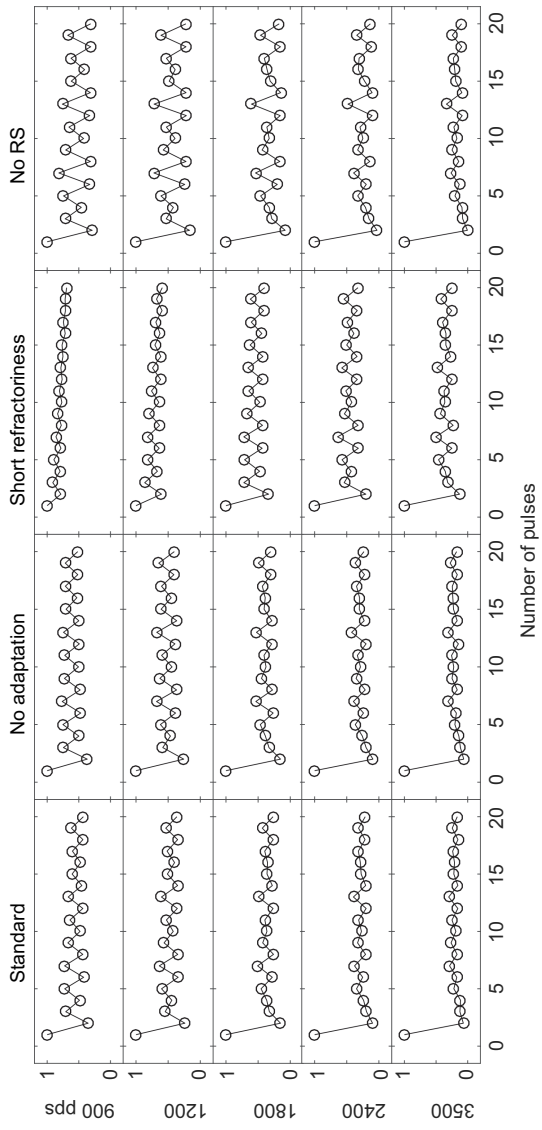

Figure 5.5. Simulations of eCAPs in response to different pulse rates. Responses to the first 20 pulses are plotted. The first column shows results obtained with the standard model parameters, the second column without adaptation, third column with short refractoriness and the fourth with deterministic parameter settings (without relative spread).

The average eCAP alternation depth and relative eCAP amplitude for each of the model parameter settings are shown in figure 5.6 for stimulation with 1.5-mA pulse trains. The results are plotted as lines overlaying the figure published by Hughes et al. (2012). By changing neural parameters, the predicted alternation depth and amplitude exhibit variability similar to that seen in the experimental data. As visible in figure 5.6A, the maximum alternation depth occurred from 900 to 1800 pps with the standard model parameters, which matches the human data. In both the human and simulated data, the alternation depth decreased when stimulated with rates of 2400 and 3500 pps. Removal of RS shifted the eCAP alternation depth at all stimulus rates tested. Both the standard parameter set and the sets with adjusted threshold stochasticity exhibited response amplitudes within the range of one standard deviation of the human data. Decreasing the refractory period increased the rate at which maximum alternation depth was visible from 900 pps in the standard model to 1800 pps, which matches the human data better. However, with this decrease the alternation depth was underestimated at 900 pps and overestimated at the highest two stimulation rates. Figure 5.6B shows that the normalized eCAP response amplitudes decreased with rates in all simulation modes, as well as in the human data. Increasing and decreasing the refractory periods caused a decrease and increase, respectively, in the normalized amplitude for all rates. Changing the adapting behavior of the neuron did not change the alternation depth or amplitude in these short duration experiments and was therefore not plotted in figure 5.6.

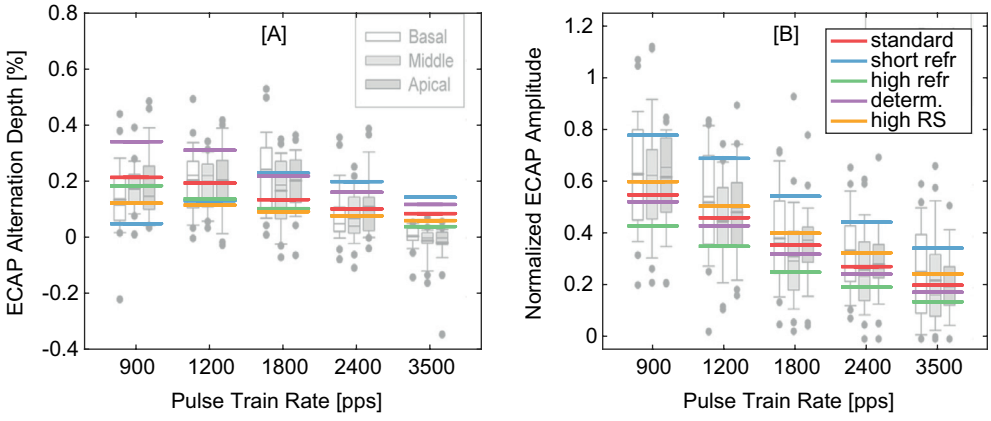

Figure 5.6. Average alternation depths [A] and eCAP amplitudes [B] for a stimulus amplitude of 1.5 mA. Normalization is achieved by dividing the eCAP amplitudes by the amplitude in response to the first pulse. Colors indicate the model setting used. Background image in grayscale shows the human data published by Hughes et al. (2012). Reprinted with permission

3.2 Experiment B: Short-duration, low-rate, pulse trains

In figure 5.7 the results obtained with the standard parameter settings and two different stimulus amplitudes (1.2 and 1.5 mA) are compared. Both amplitudes evoked eCAP modulations similar to the lower range of modulations seen in human data by Carlyon and Deeks (2015). Some patients' eCAP responses exhibited much larger alternations, up to 30% at 500 pps. This could be achieved in the model by increasing the refractory periods, or by using a deterministic model by omitting the threshold stochastics. The removal of threshold adaptation of the neuron did not change the predicted alternation amplitudes. The modulation amplitude increased with refractory period at low stimulus rates. It decreased at short refractory periods compared to the standard parameter setting, as similarly seen for the low rates in figures 5.5 and 5.6. The minor differences in alternation amplitude between the 900-pps simulations in figure 5.6 and 5.7 can be explained by the fact that stimulus levels and durations slightly differed. This was necessary because we intended to replicate the experiments performed in human subjects

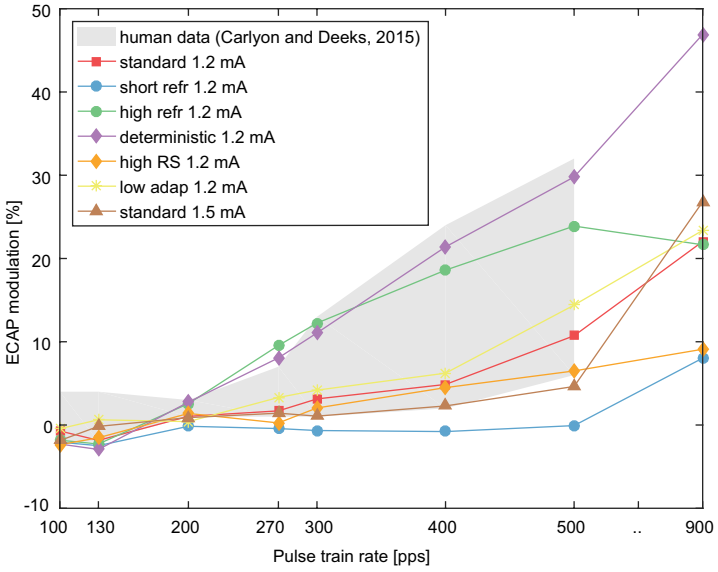

Figure 5.7. Percentage eCAP modulation in simulated responses to 100-ms pulse-trains. Responses predicted to 100, 130, 200, 270, 300, 400, and 500 pps for two different stimulus levels and varied parameter settings, which were compared to human data from Carlyon and Deeks (2015), which appears in grey as a reference. Also, stimulations with 900 pps are included to allow comparison with the data by Hughes et al (figure 5.6).

3.3 Experiment C: Long-duration pulse trains

Figure 5.8A-C show simulated normalized responses to 1.2-mA, constant-amplitude, pulse trains, at the last 10 pulses of stimulation. Results for the standard parameter setting and two model settings, namely one with longer refractory periods and one where the adaptation property was removed from the model, are shown in the respective figure 5.8A-C. Figure 5.8B shows that elongating the refractory periods by multiplication with a factor of 1.5 did change the eCAP response pattern by less than 10% compared to the standard parameter setting. The average eCAP amplitude at the end of the pulse train was slightly lower at longer refractory periods than in the standard parameter setting. Removal of adaptation (figure 5.8C) caused more alternation at the end of the pulse train for pulse rates of 500 to 1250 pps. The average response amplitude increased up to about 100% when adaptation was removed (e.g. 1667 pps, figure 5.8C). Both increased eCAP alternation and increased eCAP amplitude were also seen in the animal data after deafening (figures 5.8E and F). Figure 5.8D shows the predicted alternation amplitudes for the three different model settings, when stimulated with different IPIs. The largest alternation was seen when the adaptation property was removed (yellow line). Figure 5.8G shows the measured maximum alternation on a group level, where the largest alternations are visible after 6 weeks of deafening (black line).

Removal of RS also led to increased alternation amplitudes, but with average response amplitudes comparable to the situation with RS set as in the standard parameter setting. Unlike these predictions, data from deafened animals showed an increased normalized response amplitude at the end of the pulse train. Runtimes of the action potential, as investigated by inclusion of latency and jitter, as well as the number of fibers, did not affect the shape of the pulse-train eCAPs.

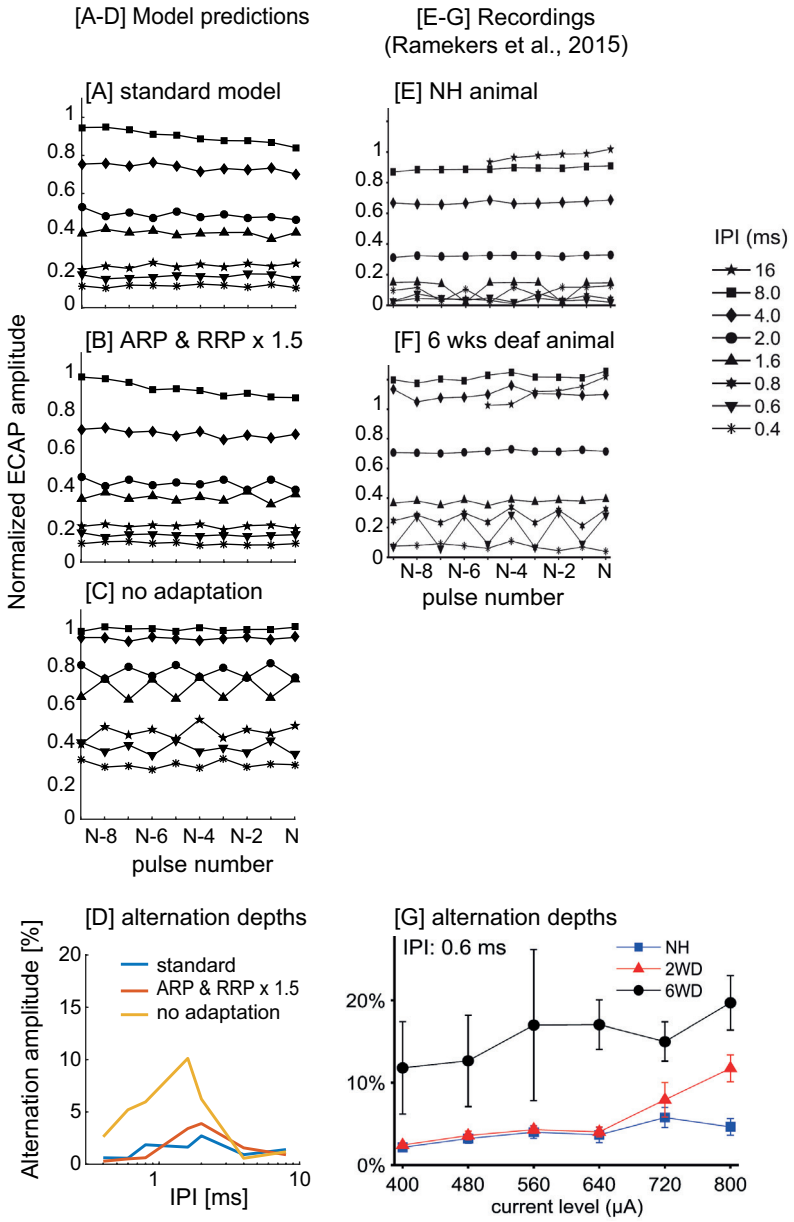

Figure 5.8. Effect of temporal properties on eCAPs in 100-ms pulse trains. [A-D] model predictions [A] Results obtained with the model with standard parameters. [B] Results obtained with elongated refractory periods or [C] without adaptation. Stimulus amplitude was 1.2 mA. [D] alternation amplitudes for the three different model perturbations at different IPI's [E-G] experimental data by Ramekers et al. (2015), reprinted with permission [E] experimental results obtained in a normal-hearing guinea pig [F] experimental results obtained in the same guinea pig, six weeks after deafening [G] group results of the average alternation in normal-hearing, 2 weeks deaf and 6 weeks deaf guinea pigs, observed at an IPI of 0.6 ms, plotted as a function of stimulus amplitude.

3.4 Experiment D: Long-duration amplitude-modulated pulse trains

The responses to amplitude-modulated pulse trains of long duration are shown in figure 5.9. Note that, in these responses, the absolute amplitudes are evaluated, whereas previous simulations looked at relative decreases in amplitude.

Modulation is followed correctly in both the experiments and the simulations. With the standard parameters, simulated responses exhibited similar behavior as in the animal experiments. However, using the standard parameter setting the eCAP amplitude never came as close to zero as the data, especially not when stimulated with the lower modulation rates. This stronger decrease in eCAP amplitude in experimental data was only replicated by the model when a strong adaptation was included, as visible in figure 5.9C. Increasing the refractoriness yielded slightly lower eCAP responses over the course of the stimulus, and a larger initial decrease in eCAP amplitude. Changing the RS had no visible effect on the eCAPs in response to amplitude-modulated pulse trains (data not shown).

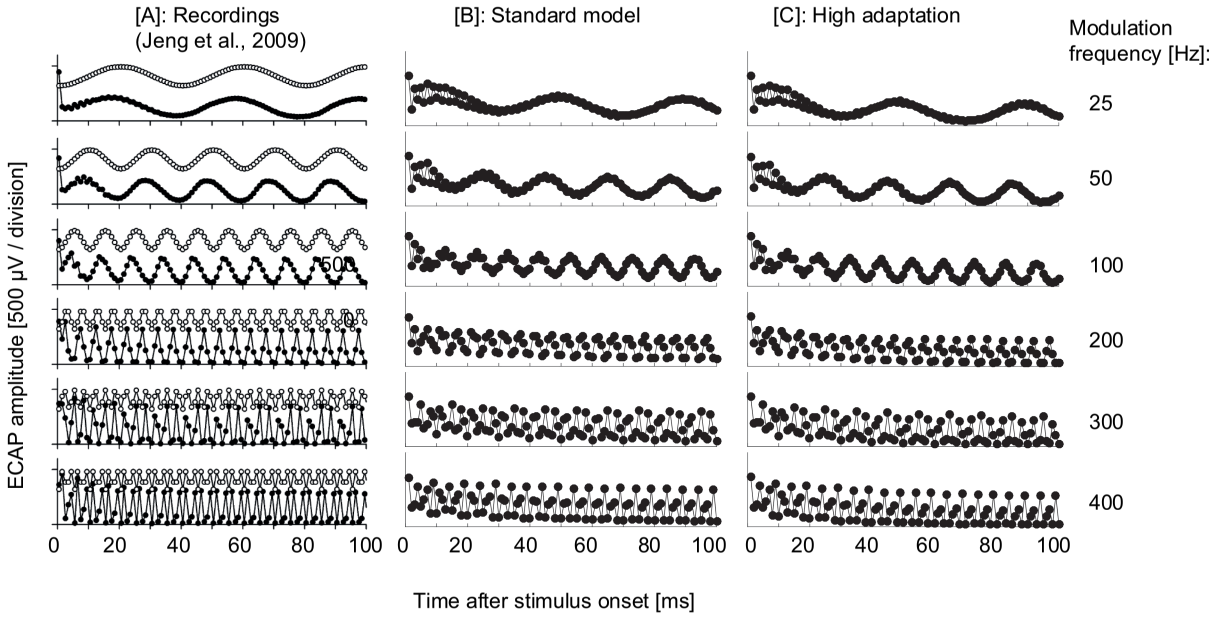

Figure 5.9. eCAP amplitudes in response to pulse trains with 10% modulation depth and modulation frequencies of 25, 50, 100, 200, 300, and 400 Hz. [A] Animal data published by Jeng et al. (2009). Reprinted with permission. The closed circles show the eCAP responses to stimuli in the amplitude-modulated pulse train. The open circles show the predicted eCAP responses based on a model without inter-pulse and stochastic effects. [B] Modeled predictions using the standard parameter settings (1.5 mA). [C] Modeled predictions with strong adaptation (1.5 mA).

3.5 Experiment E: Short-duration amplitude-modulated pulse trains

Simulated MRAs in response to pulse trains modulated with different frequencies and modulation depths are plotted in figure 5.10. The simulated responses show an increased MRA with modulation frequency and modulation depth, which was also observed in human data (Tejani et al., 2017). Stimulus level and the number of fibers modeled largely influenced the MRA, with more fibers and larger pulse amplitudes leading to larger MRAs. Variation of adaptation and RS parameters did not affect the responses. The only parameter that, though to a small extend, affected the response was the refractoriness, with a shorter refractoriness leading to larger MRAs, which was best seen at the lower modulation frequencies. All model settings are physiologically viable based on a comparison to human data from Tejani et al (2017).

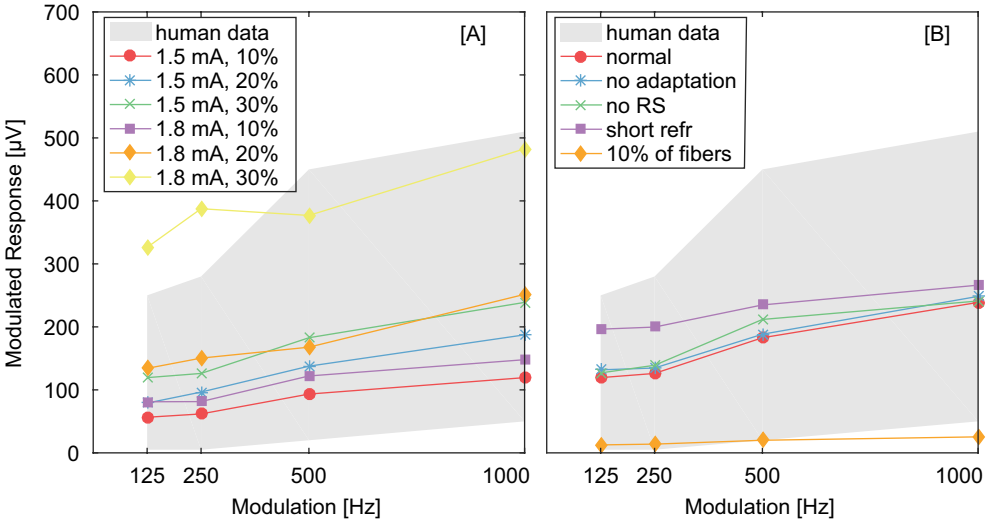

Figure 5.10. Modulated response amplitudes to modulated pulse trains with modulation frequencies of 125, 250, 500, and 1000 Hz. [A] Effect of stimulus amplitude and modulation depth. Modulation depths were varied from 10 to 20 and 30%, with mean amplitudes of 1.2 and 1.5 mA. [B] Effect of neural parameters. MRA responses obtained with standard and adjusted parameter settings are shown. Grey areas indicate the data as obtained from human experiments by Carlyon and Deeks (2015).

4 Discussion

Predicted pulse-train eCAP responses to both short- and long-duration stimuli and both animal and human studies were validated by comparison to different sets of measurement data (Carlyon and Deeks, 2015; Hughes et al., 2012; Jeng et al., 2009; Ramekers et al., 2015; Tejani et al., 2017). The model predictions were reproducible with variation of the temporal and stochastic behavior of the nerve within physiological ranges, explaining the large inter-patient variability in experimental studies (Hay-McCutcheon et al., 2005; Huarte et al., 2014; Hughes et al., 2014, 2012; McKay et al., 2013; Wilson et al., 1997, 1994; Zhang et al., 2013). Different aspects of eCAP responses to pulse trains were predicted. The main findings of the study are that, for constant-amplitude stimuli, refractoriness affects the frequency of maximum alternation, RS affects the maximum depth of the alternation, and adaptation affects the average response amplitude and alternation depth after long durations of stimulation. As we hypothesized, the eCAP responses to pulse trains were related to adaptation, as simulations with diminished adaptation explained data obtained from deafened animals. Thus, the model showed that patterns in the eCAP response to pulse trains provide insight into both the temporal and stochastic nature of the auditory nerve. The model, as a tool of interpretation, provides additional insights into the temporal and stochastic behavior of the nerve, which is expected to be related to auditory performance in patients with a CI, from pitch discrimination and amplitude modulation detection to speech perception.

Model validation with human data

Experiments A and B show that on a group level, all eCAP alternation depth predictions are within the range of physiological data for short duration stimulation with rates up to 2400 pps. For the highest rate simulations, the short refractory and deterministic setting predict a too large alternation depth. Our predictions of eCAP alternation depths were unaffected by the inclusion of latency and jitter. The latency merely caused a slightly delayed response. Spike jitter, or variability in spike timing, can theoretically cause smaller eCAP amplitudes, due to reduced synchronous fiber responses. However, the included mean jitter was approximately 70 µs and the unitary response width approximately 1 ms, and hence the jitter effect was predicted to be too small to be visible in the predictions. Overall, we conclude that our standard parameter settings, or longer refractory periods combined with a larger stochasticity, would describe the group behavior of the alternation depth best.

In both short duration experiments (A and B), the eCAP amplitudes as predicted by the standard parameter settings are well within the standard variation of patient data. The final amplitude was lower when higher stimulus rates were used. This steeper decrease has been attributed to adaptation and accommodation (Hughes et al., 2012). Our model shows however that removal of adaptation did not affect the final amplitude in the short-duration, high-stimulation-rate, experiments, but was merely dependent on the refractoriness.

Our simulations show that the nerve's refractory period alters the rate at which the maximum alternation is seen; with larger refractory periods, the stimulus rate at which the alternation depth is largest decreases. Two-pulse-eCAP paradigms provide a measure of the mean refractory behavior of an auditory nerve (Miller et al., 2001). On the basis of the results presented here, we provide an alternative method for deducing the refractory behavior of the nerve. To apply this alternative method, the alternation depth has to be measured as a function of pulse rate per individual, and not averaged over the group as in the study by Hughes et al. (2012). By finding the stimulus rate at which the eCAP alternation is maximal, the average refractory period of the nerve can be estimated. After obtaining jitter, RS and refractory periods, by using long duration stimulations for the same fiber, also a value for adaptation can be estimated.

Neural behavior and short duration pulse-train eCAP responses

As mentioned, the implemented variations of parameters describing the neural behavior result in a variability in pulse-train eCAPs similar to that seen in human data. The underlying biophysical phenomena causing differences in eCAP responses could be related to size, myelination and the number of sodium channels in the auditory nerve. Neuronal degeneration that follows deafness leads to axonal shrinkage, demyelination and a progressive retraction of the peripheral axon (Leake and Hradek, 1988). Stochasticity, or the RS of the threshold, was shown in a model study to depend on the myelination of the nerve, with demyelination reducing RS (Resnick et al., 2018), though in another study no relation between deafness and dynamic range of the auditory neurons was found (Sly et al., 2007). Our model showed that decreased stochasticity (i.e. reduced RS) of the nerve can lead to increased alternation depths independent of stimulus rate. Several studies have shown that refractory periods are longer in animals with hearing loss than in control animals (Rubinstein, 1995; Shepherd et al., 2004; Shepherd and Javel, 1997; Sly et al., 2007; Walton et al., 1995; Waxman and Ritchie, 1993). Prolonged refractory time-constants have been observed in demyelinated neurons (Waxman and Ritchie, 1993), of which the chronically deafened auditory nerve is an example (Leake and Hradek, 1988). Demyelinated nerve fibers have relatively fewer potassium channels, which might result in a leakage of internodal potassium currents into the nodal regions and thus cause a prolongation of refractory time constants. Our simulations show that increased refractoriness and decreased stochasticity can cause this increase in eCAP modulation. Thus, measurement of the pulse-train eCAP alternation could provide a measure related to hearing loss. A psychophysical study by Carlyon and Deeks (2015) showed that patients with larger alternation depths in their eCAP responses performed worse on rate discrimination tasks. Our data suggests that patients with better rate discrimination have auditory neurons with short refractory periods and strong stochastic behavior.

Neural behavior and long duration pulse-train eCAP responses

Our model shows that a decrease in adaptation magnitude produced the increased alternation of eCAP amplitude and response amplitude as seen in deafened guinea pigs in the study of Ramekers et al (2015). In their study an increased alternation depth

of pulse-train eCAP in chronically deafened animals was hypothesized to be related to altered refractoriness or jitter in hearing impaired animals. Our study shows that the only parameter adjustment that can cause both the increased alternation depth and increased eCAP amplitude is removal of adaptation. Some earlier studies investigated the relationship between hearing loss and neural adaptation in both animals and humans, and attempted to investigate the relationship between adaptation and deafness on different neural levels (Abbas, 1984; Haenggeli et al., 1998; Kidd et al., 1984; Kotak, 2005; Scheidt et al., 2010; Walton et al., 1995; Wojtczak and Oxenham, 2010; Xu et al., 2007; Xu and Collins, 2007; Zhang et al., 2010). Apart from the study by Ramekers et al. (2015) there are to our knowledge no other studies that describe the relation between hearing loss and pulse-train eCAP alternation depth in response to long-duration pulse trains. Such data could be extracted from existing studies. For example, from the study by Hay-McCutcheon et al. (2005) the adaptation could be calculated as the final decrease versus the initial decrease in eCAP amplitude, and subsequently be related to deafness.

Neural behavior and MRA

The MRA was suggested by Tejani et al. (2017) to be related to neural adaptation. However, changing the adaptation parameter in our model did not affect the predicted MRAs, suggesting that the MRA in response to these stimuli is not a good measure of the nerve's adaptive behavior. The only neural parameter variation that, and only to a small extend, affected the MRA was the refractory period. Electrophysiological recordings of chicken auditory nerve fibers have shown that refractoriness in the auditory nerve potentially enhances entrainment in response to sound stimuli and, thus, is important for temporal coding (Avissar et al., 2013). Our simulations confirmed these conclusions, as the simulation with shorter refractory periods yielded larger MRAs, implying that longer refractoriness due to hearing loss causes lower modulation response amplitudes. As amplitude modulations are important aspects of speech, we hypothesize that the increased refractory periods lead to lower modulation response amplitudes and decrease the intelligibility of speech for CI users. However, as Tejani et al. showed, the MRA increases with modulation frequency, whereas the psychophysical measure of modulation detection deteriorates. This suggests that more central factors also play a role, possibly limiting the detection of amplitude modulations. The modeled MRA responses were unaffected by adaptation or RS. ECAP responses to amplitude-modulated stimulation slightly depend on the nerve's behavior (refractoriness), but are more strongly affected by the stimulus modulation-depth and frequency. No model perturbation reproduces the large modulation response amplitude at 500 and 1000 Hz modulation reported by Tejani et al. (2017). The patient showing the largest MRA was also stimulated with the largest modulation depth, 35%. An additional simulation, with this modulation depth, yielded an MRA of around 500 μV for 1000 Hz modulation, very similar to the experimental results. Therefore, we conclude, in line with the observations by original authors, that there is a strong correlation between the MRA and modulation depth (Tejani et al., 2017), and that interpatient differences in MRA are mostly a consequence of modulation depth and stimulus amplitude used rather than the neuronal status.

Model improvements

In some experiments, increased eCAP amplitudes over the stimulus duration were observed (He et al., 2015). This is thought to be caused by integration effects, which were not included in our current model. Huarte et al. (2014) and Schmidt, Clay, and Brown (2007) recorded eCAPs in response to minute-long stimulations in humans and saw the eCAP amplitude decrease over longer periods of time. To reproduce such long-term effects, temporal adaptation components longer than 100 ms will have to be included in the model or be modeled using a power-law as shown previously for the response of auditory neurons to sound (Zilany and Carney, 2010).

The unitary response used is based on cat data (Miller et al., 1999b). We have repeated all our simulations with the unitary response published by Versnel et al. (1992). These altered simulations did not yield changes in the predicted normalized pulse-train eCAP responses. Some studies suggest that the unitary response is an oversimplification of the actual contribution to the eCAP for all different fibers, especially for high stimulation levels (Briaire and Frijns, 2005; Westen et al., 2011). Doucet and Relkin (1997) showed that when the total area of neural activation spans more than three octaves, location effects also become significant. A more elaborate version of our 3D model could be used to study this issue in more detail. Not only the exact site of activation can be predicted using the active cable model, but also the propagation of the action potentials along these fibers, and their contribution to the SFAP (Briaire and Frijns, 2005). Differences in fiber kinetics, neuron myelination, size, and morphology between the cochleae of different species influence the shape of the unitary response. An important factor is for instance that in humans the soma is unmyelinated, which effectively adds a large capacitance to the human auditory nerve, leading to altered spike propagation times along the nerve. For prediction of the human eCAP, a unitary response derived especially for the human situation would be desirable. Deconvolution of the human eCAP with modeled predictions of the spike responses, including latency distributions, can provide insight into the variations in the contributions of different human auditory nerve fibers (Schoonhoven, Stegeman, and van Oosterom, 1988). One could potentially use a deconvolution method as suggested by Strahl et al. (2016), to include the optimization of the shape of the human unitary response while fitting recorded human eCAP data (Dong et al., 2018). The active cable model used in the current paper contains a human morphology, described as the new human soma, combined with GSEF kinetics (Kalkman et al., 2015). Kinetics more based on the human situation as described by Schwarz and Reid (Schwarz et al., 1995) are being implemented in a newer double cable version of the model that we hope to use in future research.